







# Synthesis of benzhydrol analogues based on 1'-acetoxychavicol acetate (ACA), as a stable and potent antiproliferative agent on breast cancer cell lines, ADMET analysis and molecular docking study

Mohamad Nurul Azmi <sup>1\*</sup>, Cheong Siong Tan <sup>1</sup>,  
Hassan Taiye  Abdulameed <sup>2,3</sup>, Nik Nur Syazni Nik Mohamad Kamal <sup>2</sup>,  
Nur Ezzah Abdul Kahar <sup>4</sup>  and Mohammad Tasyriq Che Omar <sup>5</sup>

<sup>1</sup>Natural Products and Synthesis Organic Research Laboratory (NPSO), School of Chemical Sciences, Universiti Sains Malaysia, 11800 Minden, Penang, Malaysia

<sup>2</sup>Advance Medical and Dental Institute, Universiti Sains Malaysia, 13200 Kepala Batas, Penang, Malaysia

<sup>3</sup>Department of Biochemistry, Kwara State University, PMB1530 Malete, Nigeria.

<sup>4</sup>Science and Engineering Research Centre (SERC), Engineering Campus, Universiti Sains Malaysia, 14300 Nibong Tebal, Penang, Malaysia

<sup>5</sup>Biological Section, School of Distance Education, Universiti Sains Malaysia, 11800 Minden, Penang, Malaysia

(Received May 24, 2024; Revised June 12, 2024; Accepted June 19, 2024)

**Abstract:** Six benzhydrol analogues were successfully synthesised and evaluated for their antiproliferative effect on breast cancer cells. These compounds were designed based on the structure of 1'-acetoxychavicol acetate (ACA) and 1'-acetoxyeugenol acetate (AEA), which known for their anticancer properties. Among them, compounds **3b**, **3e**, and **3f** demonstrated significant activity against MCF-7 and MDA-MB-231 breast cancer cell lines (between 5.5-6.0  $\mu$ M and 1.1-7.0  $\mu$ M, respectively), outperforming tamoxifen as the standard control. Molecular docking studies revealed that compounds **3b**, **3e**, and **3f** shows good binding energies ranging from -5.13 to -7.27 kcal/mol with Nuclear Factor-KappaB Kinase alpha ( $\text{I}\kappa\text{B}\alpha$ ) protein (PDB ID: 1NFI), compared to -5.27 kcal/mol for tamoxifen (control). **3b** and **3f** interact with  $\text{I}\kappa\text{B}\alpha$  at several residues including APE77, VAL93, and VAL97. The SwissADME and toxicity prediction analysis indicates that three compounds (**3b**, **3e**, and **3f**) adhere to the principles of drug-likeness. These findings suggest that the benzhydrol analogues, particularly **3b**, **3e**, and **3f**, could be promising lead for further development as anticancer agents.

**Keywords:** Benzhydrol analogues; antiproliferative; breast cancer; molecular docking;  $\text{I}\kappa\text{B}\alpha$  protein. ©2024 ACG Publication. All rights reserved.

## 1. Introduction

Breast cancer is the most prevalent malignancies affecting women worldwide with 2,296,840 cases (23.8%) and 666,103 deaths (15.4%) being reported in 2022. According to GLOBOCAN 2022 report, breast cancer constitutes approximately 31.3% of diagnosed cancers and 24.1% of cancer deaths

\* Corresponding author: E-Mail: [mnazmi@usm.my](mailto:mnazmi@usm.my)

## Synthesis of benzhydryl analogues, antiproliferative activity and *in silico* studies

affecting Malaysian women.<sup>1</sup> Breast cancer consists of various biological subtypes which possess different characteristics and their treatment options. Among these subtypes, triple-negative breast cancer (TNBC) accounts for roughly 20% of all breast cancers and it is usually characterized by the expression deficiency of progesterone receptor (PR), estrogen receptor (ER) and human epidermal growth factor receptor 2 (HER2).<sup>2</sup> TNBC is regarded as a high grade breast cancer due to its aggressiveness. Moreover, TNBC does not respond to most of the targeted regimens such as HER2 monoclonal antibodies and ER antagonists. This eventually causes the number of metastatic cases and deaths to increase.<sup>3</sup> Hence, there is an urgent need to explore effective drugs for the treatment of breast cancer, particularly TNBC.

In this study, we will synthesise the benzhydryl analogues based on 1'-acetoxychavicol acetate (ACA) structure (Figure 1). ACA was previously isolated by our group from Malaysian wild-ginger, *Alpinia conchigera* Griff shows interesting cytotoxic activity on various cell lines including MDA-MB-231 (4.8  $\mu$ M), MCF-7 (30.0  $\mu$ M), RT-112 (14.1  $\mu$ M), EJ-28 (8.2  $\mu$ M), PC-3 (26.7  $\mu$ M), HSC-2 (5.0  $\mu$ M) HSC-4 (5.5  $\mu$ M), HepG2 (18.0  $\mu$ M) and CaSki (17.0  $\mu$ M).<sup>3-4</sup> ACA also represents an attractive candidate for the treatment of many diseases<sup>5</sup> and its ability to have anti-inflammatory properties.<sup>6-7</sup> The mechanism of action of ACA and its analogue (i.e 1'-acetoxyeugenol acetate, AEA) is associated with the suppression of Nuclear Factor-KappaB Kinase alpha ( $\text{I}\kappa\text{B}\alpha$ ) activation followed by the eventual inhibition of NF- $\kappa$ B activation.<sup>8-9</sup>

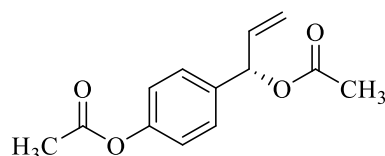


**Figure 1.** Acetoxychavicol acetate (ACA)

One of the problem for ACA, is the transformation of this compound to their isomer namely *trans p*-coumaryl acetate (TPCA, **2**) via [3,3]-sigmatropic rearrangement (Figure 2). This transformation will affect the cytotoxicity from active to not active.

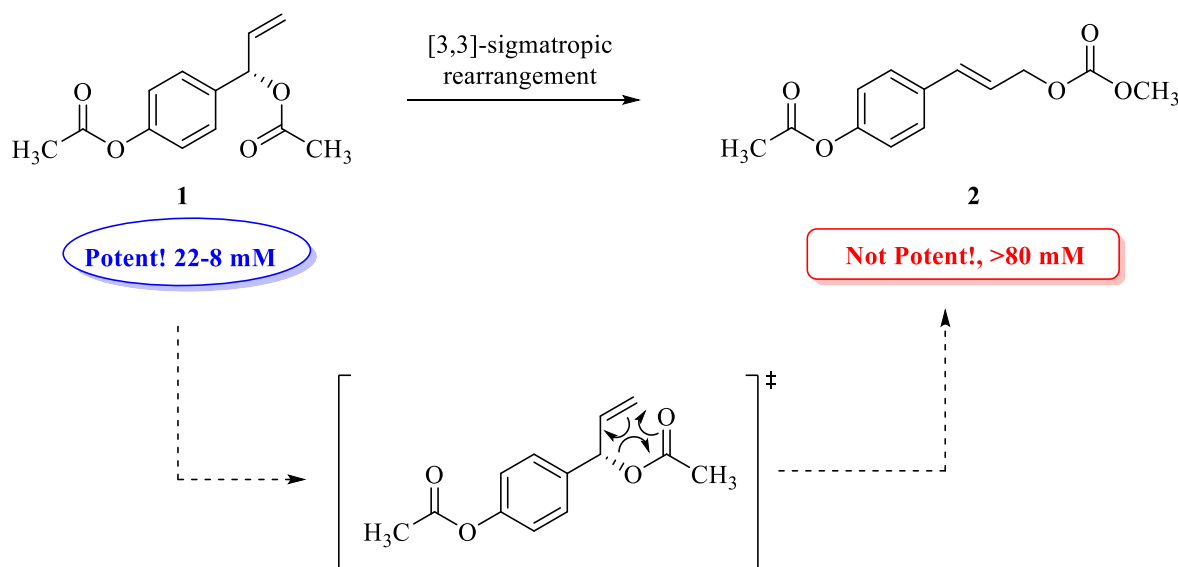


**Figure 2.** Transformation of 1'-acetoxychavicol acetate (**1**) to *trans p*-coumaryl acetate (**2**)

In this study, we will synthesise the benzhydryl analogues based on the ACA structure to address the issue of instability and also to evaluate the cytotoxicity of the compounds on the human breast cancer cell lines MCF-7 and MDA-MB-231 compared to MCF-10A, the normal human breast cell lines. The

ADMET, prediction of toxicity profile and molecular docking of potent compounds on IκBα were investigated to understand their interactions between ligand and active sites.

## 2. Experimental

### 2.1. General

All reactions were carried out in heat-dried glassware under an atmosphere of nitrogen unless otherwise stated. All liquid transfers were conducted using standard syringe or cannula techniques. DCM was dried under molecular sieves 4Å. All other reagents were obtained from Merck or Aldrich and used as received. Column chromatography was performed on silica gel (Merck, 60 Å C. C. 40-63 mm) as the stationary phase. Thin Layer Chromatography (TLC) was performed on alumina plates pre-coated with silica gel (Merck silica gel, 60 F254), which were visualized by the quenching of UV fluorescence when applicable ( $\lambda_{\text{max}} = 254 \text{ nm}$  and/or  $366 \text{ nm}$ ) and/or by spraying with vanillin in acidic ethanol followed by heating with a heat gun. NMR spectra were recorded on a Bruker Avance (500 MHz for  $^1\text{H}$  NMR, 125 MHz for  $^{13}\text{C}$  NMR) spectrometer system. Data were analysed via TopSpin 3.6.1 software package. Spectra were referenced to TMS or residual solvent ( $\text{CDCl}_3 = 7.26 \text{ ppm}$  in  $^1\text{H}$  spectroscopy, and  $77.0 \text{ ppm}$  in  $^{13}\text{C}$  spectroscopy;  $\text{MeOD-D}_4 = 4.78, 3.31 \text{ ppm}$  in  $^1\text{H}$  spectroscopy, and  $49.2 \text{ ppm}$  in  $^{13}\text{C}$  spectroscopy). Fourier transform infrared (FT-IR) spectra were recorded by Perkin Elmer FT-IR spectroscopy (Perkin Elmer, Waltham, MA, USA) in the frequency range of  $4000 - 400 \text{ cm}^{-1}$  using the ATR method. Melting points were measured using an open capillary tube by Stuart Scientific SMP10 melting point apparatus (Staffordshire, UK) in temperatures ranging from  $25 \text{ }^\circ\text{C}$  to  $350 \text{ }^\circ\text{C}$ .

### 2.2. Chemistry

#### 2.2.1. Synthesis of 4-(hydroxy(phenyl)methyl)phenol (**2**)

The 4-hydroxybenzophenone (**1**) (2.13 g, 10.76 mmol) was treated with  $\text{NaBH}_4$  (1.64 g, 43.04 mmol) in the mixture of THF (100 mL) and  $\text{H}_2\text{O}$  (30 mL). While the mixture was heated under reflux for overnight, the colour of the mixture was gradually changed from pale yellow to colourless. The reaction mixture was quenched with saturated aqueous ammonium chloride ( $\text{NH}_4\text{Cl}$ ) (20 mL). The layers were then separated and the aqueous layer was extracted with ethyl acetate (EtOAc) ( $3 \times 20 \text{ mL}$ ). The combined organic solvents were then dried over sodium sulphate ( $\text{Na}_2\text{SO}_4$ ), filtered, and collected. The product was directly used without further purification. The spectroscopic data will compared with those reported in the literature (Supporting information, S1-S2).<sup>10</sup>

#### 2.2.2. Synthesis of 4-(acetoxy(phenyl)methyl)phenyl acetate (**3a**) – Path A

A benzhydrol **2** (0.220 g, 1.10 mmol) was dissolved in 10 mL of dry dichloromethane (DCM) and stirred in an ice bath. The 4-dimethylaminopyridine (DMAP) (0.268 g, 2.20 mmol), triethylamine ( $\text{Et}_3\text{N}$ ) (0.31 mL, 2.22 mmol) and acetic anhydride (0.21 mL, 2.20 mmol) were added dropwise while stirring the reaction solution. The ice bath was removed and the mixture was allowed to stirred at room temperature. The reaction progress was monitored by TLC (1:4, *n*-hexane: ethyl acetate). After stirring at room temperature for overnight, the reaction mixture was quenched with saturated aqueous ammonium chloride ( $\text{NH}_4\text{Cl}$ ) (20 mL). The layers were then separated and the aqueous layer was extracted with ethyl acetate (EtOAc) ( $3 \times 20 \text{ mL}$ ). The combined organic solvents were then dried over sodium sulphate ( $\text{Na}_2\text{SO}_4$ ), filtered, and collected. The excess volatile solvent was removed under reduced pressure by using a rotary evaporator then gave the product as the yellowish oil (Supporting information, S3-S4).<sup>11</sup>

#### 2.2.3. General Procedure for Acylation Reactions (Path B):

A benzhydrol **2** (1.0 equiv.) was dissolved in 20 mL of dry dichloromethane (DCM) and stirred in an ice bath. The 4-dimethylaminopyridine (DMAP) (0.1 equiv.), triethylamine ( $\text{Et}_3\text{N}$ ) (0.5 equiv.)

## Synthesis of benzhydrol analogues, antiproliferative activity and *in silico* studies

and acyl chloride (2.2 equiv.) were added dropwise while stirring the reaction solution. The ice bath was removed and the mixture was allowed to stirred at room temperature for overnight. The reaction progress was monitored by TLC (1:4, *n*-hexane: ethyl acetate). After stirring at room temperature for overnight, the reaction mixture was quenched with saturated aqueous ammonium chloride (NH<sub>4</sub>Cl) (20 mL). The layers were then separated and the aqueous layer was extracted with ethyl acetate (EtOAc) (3×20 mL). The combined organic solvents were then dried over sodium sulphate (Na<sub>2</sub>SO<sub>4</sub>), filtered, and collected. The excess volatile solvent was removed under reduced pressure by using a rotary evaporator then gave the product **3** (Supporting information, S5-S14).

(Et<sub>3</sub>N) (0.31 mL, 2.22 mmol) and isobutyryl chloride (0.23 mL, 2.20 mmol) were added dropwise while stirring the 4-((benzoyloxy)(phenyl)methyl)phenyl benzoate (**3b**). A benzhydrol **2** (0.212 g, 1.06 mmol) was dissolved in 10 mL of dry dichloromethane (DCM) and stirred in an ice bath. The 4-dimethylaminopyridine (DMAP) (0.268 g, 2.20 mmol), triethylamine (Et<sub>3</sub>N) (0.31 mL, 2.22 mmol) and benzyl chloride (0.26 mL, 2.20 mmol) were added dropwise while stirring the reaction solution. The reaction then proceeded and worked up according to the general procedure.

4-((butyryloxy)(phenyl)methyl)phenyl butyrate (**3c**). A benzhydrol **2** (0.209 g, 1.05 mmol) was dissolved in 10 mL of dry dichloromethane (DCM) and stirred in an ice bath. The 4-dimethylaminopyridine (DMAP) (0.268 g, 2.20 mmol), triethylamine (Et<sub>3</sub>N) (0.31 mL, 2.22 mmol) and butyryl chloride (0.25 mL, 2.20 mmol) were added dropwise while stirring the reaction solution. The reaction then proceeded and worked up according to the general procedure.

4-((isobutyryloxy)(phenyl)methyl)phenyl isobutyrate (**3d**)<sup>11</sup>. A benzhydrol **2** (0.220 g, 1.10 mmol) was dissolved in 20 mL of dry dichloromethane (DCM) and stirred in an ice bath. The 4-dimethylaminopyridine (DMAP) (0.268 g, 2.20 mmol), triethylamine reaction solution. The reaction then proceeded and worked up according to the general procedure.

4-(((cyclohexanecarbonyl)oxy)(phenyl)methyl)phenyl cyclohexane carboxylate (**3e**). A benzhydrol **2** (0.220 g, 1.10 mmol) was dissolved in 20 mL of dry dichloromethane (DCM) and stirred in an ice bath. The 4-dimethylaminopyridine (DMAP) (0.268 g, 2.20 mmol), triethylamine (Et<sub>3</sub>N) (0.31 mL, 2.22 mmol) and cyclohexanecarbonyl chloride (0.26 mL, 2.20 mmol) were added dropwise while stirring the reaction solution. The reaction then proceeded and worked up according to the general procedure.

4-(((furan-2-carbonyl)oxy)(phenyl)methyl)phenyl furan-2-carboxylate (**3f**). A benzhydrol **2** (0.220 g, 1.10 mmol) was dissolved in 20 mL of dry dichloromethane (DCM) and stirred in an ice bath. The 4-dimethylaminopyridine (DMAP) (0.268 g, 2.20 mmol), triethylamine (Et<sub>3</sub>N) (0.31 mL, 2.22 mmol) and 2-furoyl chloride (0.22 mL, 2.20 mmol) were added dropwise while stirring the reaction solution. The reaction then proceeded and worked up according to the general procedure.

### 2.3. Biological Assay

#### 2.3.1. Cell Cultures

MCF-7 and MDA-MB-231 human breast cancer cell lines, as well as MCF-10A, human normal breast cell lines, were used in this study. These cells were acquired from the American Type Culture Collection (Manassas, VA, USA). MCF-7 and MDAMB-231 cells were regularly cultured in Dulbecco's Modified Eagle's Medium (DMEM; Gibco, Waltham, MA, USA), and supplemented with 10% (*v/v*) fetal bovine serum (FBS; Gibco, Waltham, MA, USA) and 100 U/mL penicillin-streptomycin (PenStrep; Gibco, Waltham, MA, USA). MCF-10A cells were routinely cultured in DMEM/F12 (Gibco, Waltham, MA, USA) medium supplemented with 5% horse serum (Sigma-Aldrich, Burlington, MA, USA), 10 µg/mL of insulin (Sigma-Aldrich, Burlington, MA, USA), 20 ng/mL of human epidermal growth factor (hEGF; ThermoFisher, Waltham, MA, USA), 0.5 µg/mL of hydrocortisone (Sigma Aldrich, Burlington, MA, USA) and 1 U/mL PenStrep. All cell lines were maintained in a humidified atmosphere with 5% CO<sub>2</sub> at 37 °C.

### 2.3.2. Antiproliferative Evaluation of Acyl Benzhydrol Analogues

The effects of the benzhydrol analogues on MCF-7, MDA-MB-231, and MCF-10A were determined using a 3-(4,5-dimethylthiazol-2-yl)-2,5-diphenyltetrazolium bromide (MTT) proliferation assay. The cells were seeded at a density of  $1 \times 10^4$  cells/well in a 96-well plate. MCF10A was used as normal cell lines to determine the selectivity index (SI) values. The cells were treated using freshly prepared medium supplemented with an increasing concentration of tested compounds (0-100  $\mu\text{g/mL}$ ) within 24-72 hours at 37 °C. For this assay, the blank and negative controls used were the culture medium alone (without cells) and cells with culture medium only (untreated cells), respectively. For the positive control, tamoxifen was used and treated at the tested concentration above. At each incubation period, 10  $\mu\text{L}$  (5 mg/mL) of MTT were added into each well, and incubated for 4 hours at 37 °C, 5%  $\text{CO}_2$ . The solution mixture in each well was replaced with 100  $\mu\text{L}$  of dimethyl sulfoxide (DMSO) to solubilize the MTT crystalline products. The optical density (O.D.) of each well was measured using a microplate reader (PowerWave-XS; Bio-Tek Instruments, Winooski, Vermont, USA) at 570 nm

### 2.3.3. Statistical Analysis

The experiments were conducted in triplicate for each cell line. A plot of % cell proliferation versus sample concentration was used to show the 50% inhibitory concentration ( $\text{IC}_{50}$ ). The selectivity index (SI) values were calculated as the ratio of the 50% cytotoxic concentration ( $\text{IC}_{50}$  in cancer cell line) to the 50% cytotoxic concentration on the normal cell line ( $\text{IC}_{50}$  in non-cancerous cell line). Values of  $*p < 0.05$  were considered significant.

## 2.4. ADMET

Determining ADME is crucial. The ADME criteria, based on Lipinski's rule of five, assess whether a ligand can be developed into a drug.<sup>12</sup> Compounds **3b**, **3d**, **3e**, and **3f**, which showed the lowest binding energies with  $\text{I}\kappa\text{B}\alpha$ , underwent analysis for physicochemical properties and ADME profiling via the SwissADME webserver.<sup>13</sup> Toxicity evaluations were conducted using the ProtoxII webserver.<sup>14</sup>

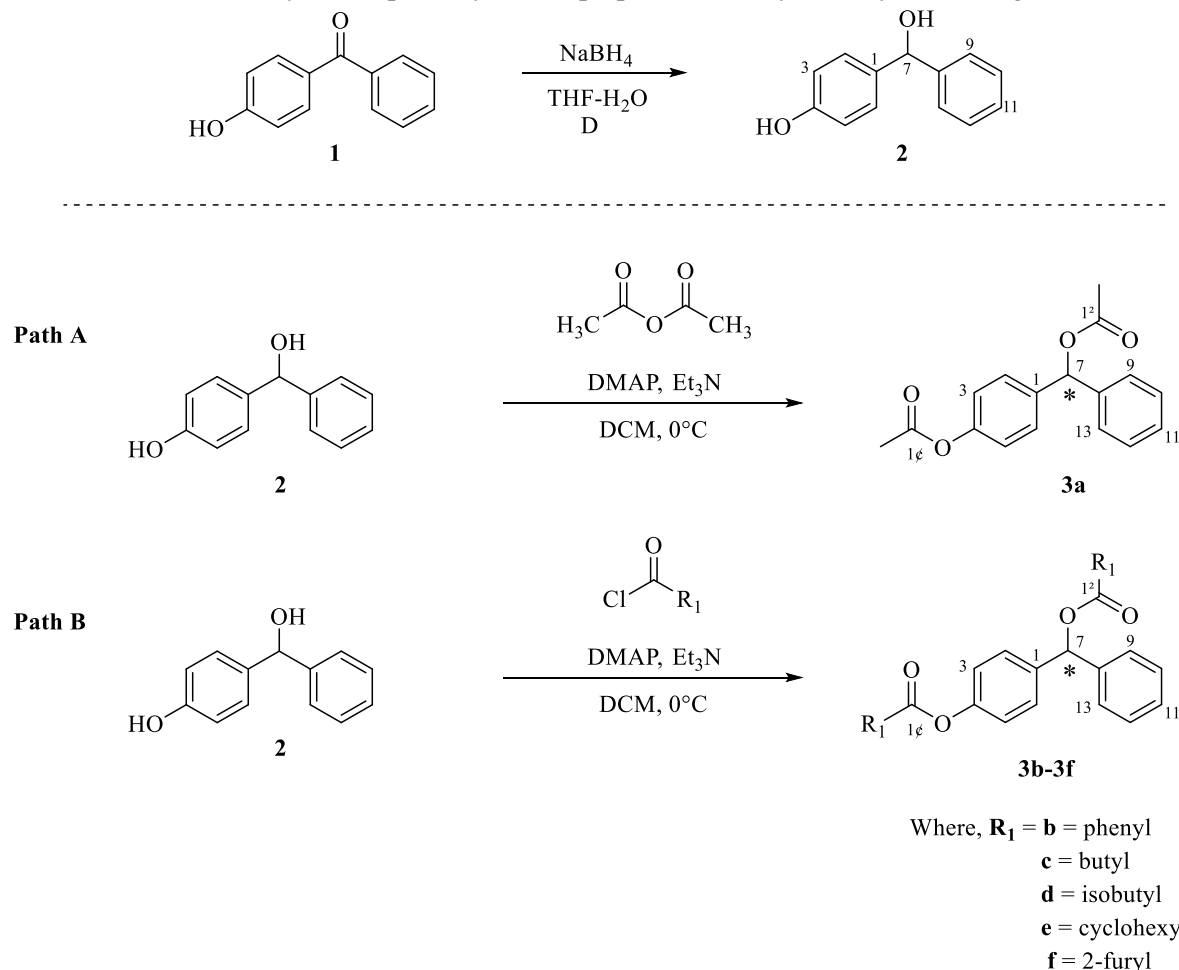
### 2.4. Molecular Docking

The binding energy of potent compounds for human Inhibitor of Nuclear Factor-KappaB Kinase alpha ( $\text{I}\kappa\text{B}\alpha$ ) were examined via molecular docking study. The procedure started with processing the PDB ID: 1NFI. The water molecules, chain a, chain b, chain c, chain d and chain F were removed using UCSF Chimera version 1.14 and saved as PDB format and named as  $\text{I}\kappa\text{B}\alpha$ .pdb. The docking is initialized by using the target compounds smiles from Chemdraw and converted the format to PDB, followed by visualising  $\text{I}\kappa\text{B}\alpha$ .pdb and compound pdbs in UCSF Chimera version 1.14.<sup>15</sup> The polar hydrogens and Gasteiger charges were added to minimize the structures in the steepest descent step. The grid size was set to 27, 38, and 39 along the X-, Y-, and Z-axes with a 0.375 Å grid spacing while the grid centre along the X-, Y-, Z-axes was set to -5.9, 81, and 59 Å for docking searching process. This box is a location where few of N-terminal of  $\text{I}\kappa\text{B}\alpha$  residues interact with NF- $\kappa\text{B}$  molecules. Lastly, the bindings and energy scores were calculated via AutoDock Vina performed in three different computers.<sup>16</sup> For further analysis, the binding interaction between protein and compounds were analysed through Biovia Discovery Studio Visualizer Client 2020 (Dassault Systèmes BIOVIA, Discovery Studio Modeling Environment, Release 2017, San Diego: Dassault Systèmes, 2016).

### 3. Results and Discussion

#### 3.1. Chemistry

**Scheme 1.** Synthetic pathway for the preparation of acyl benzhydropol analogues



Scheme 1 shows the route for the preparation of six benzhydropol analogues **3a-3f**. The benzhydropol analogues were synthesised from the intermediate **2**, which was prepared from reduction of 4-hydroxybenzophenone (**1**) using sodium borohydride (Scheme 1). Treatment of **2** with acetic anhydride under usual condition afforded the acetyl analogue **3a** (Path A) in 70% yield. Meanwhile the acyl analogues (i.e **3b-3f**) were prepared by acylation of **2** with respective acyl chlorides in the presence of triethylamine and dimethylaminopyridine at 0°C afforded good yield products between 85-91% (Path B). All synthesise compounds were elucidated using spectroscopic methods.

*4-(hydroxy(phenyl)methyl)phenol (2)*: White solid. Yield: (2.14 g, 99%). IR ( $\tilde{\nu}/\text{cm}^{-1}$ ):  $^1\text{H}$  NMR (500 MHz,  $\text{CD}_3\text{OD}$ ,  $\delta/\text{ppm}$ ): 4.48 (br s, 1H, O-H), 5.63 (s, 1H, H-7), 6.69 (d,  $J = 8.6$  Hz, 2H, H-3, H-5), 7.09 (d,  $J = 8.6$  Hz, 2H, H-2, H-6), 7.14 (t,  $J = 7.5$  Hz, 1H, H-11), 7.24 (t,  $J = 7.5$  Hz, 2H, H-10, H-12), 7.28 (d,  $J = 7.5$  Hz, 2H, H-9, H13).  $^{13}\text{C}$  NMR (125 MHz,  $\text{CD}_3\text{OD}$ ,  $\delta/\text{ppm}$ ): 76.8 (C-7), 116.1 (C-3, C-5), 127.7 (C-9, C13), 128.1 (C-11), 129.3 (C-2, C-6, C-10, C-12), 137.0 (C-1), 146.4 (C-8), 157.9 (C-4).

*4-(acetoxymethyl)phenyl phenyl acetate (3a)*: Orange oil. Yield: (0.87 g, 70%). IR ( $\tilde{\nu}/\text{cm}^{-1}$ ): 3021 (Csp<sup>2</sup>-H stretching), 1711 (C=O stretching), 1510, 1223 (C-O stretching), 746.  $^1\text{H}$  NMR (500 MHz,  $\text{CDCl}_3$ ,  $\delta/\text{ppm}$ ): 2.16 (s, 3H, H-2''), 2.29 (s, 3H, H-2'), 6.89 (s, 1H, H-7), 7.06 (d,  $J = 8.6$  Hz, 2H, H-3, H-

5), 7.27-7.35 (m, 7H, H-2, H-6, H-9–H-13).  $^{13}\text{C}$  NMR (125 MHz,  $\text{CDCl}_3$ ,  $\delta/\text{ppm}$ ): 21.2 (C-2'), 21.3 (C-2''), 76.3 (C-7), 121.6 (C-3, C-5), 127.0 (C-9, C-13), 128.0 (C-11), 128.4 (C-2, C-6), 128.6 (C-10, C-12), 137.8 (C-1), 139.9 (C-8), 150.2 (C-4), 169.5 (C-1'), 170.0 (C-1'').

4-((benzoyloxy)(phenyl)methyl)phenyl benzoate (**3b**): White solid. Yield: (0.38 g, 85%). IR ( $\tilde{\nu}/\text{cm}^{-1}$ ): 3021 (Csp<sup>2</sup>-H stretching), 1725 (C=O stretching), 1211 (C-O stretching), 743.  $^1\text{H}$  NMR (500 MHz,  $\text{CDCl}_3$ ,  $\delta/\text{ppm}$ ): 7.08 (s, 1H, H-7), 7.14 (d,  $J = 8.7$  Hz, 2H, H-3, H-5), 7.23 (t,  $J = 7.3$  Hz, 1H, H-11), 7.30 (t,  $J = 7.3$  Hz, 2H, H-10, H-12), 7.38-7.44 (m, 8H, H-2, H-6, H-9, H-13, H-4', H-6', H-4'', H-6''), 7.51 (t,  $J = 7.3$  Hz, 1H, H-5''), 7.55 (t,  $J = 7.3$  Hz, 1H, H-5'), 8.08 (d,  $J = 8.5$  Hz, 2H, H-3'', H-7''), 8.11 (d,  $J = 8.5$  Hz, 2H, H-3', H-7').  $^{13}\text{C}$  NMR (125 MHz,  $\text{CDCl}_3$ ,  $\delta/\text{ppm}$ ): 76.9 (C-7), 121.8 (C-3, C-5), 127.2 (C-9, C-13), 128.1 (C-11), 128.5 (C-4', C-6', C-4'', C-6''), 128.6 (C-2, C-6), 128.6 (C-10, C-12), 129.4 (C-2''), 129.8 (C-3'', C-7''), 130.1 (C-2'), 130.2 (C-3', C-7'), 137.9 (C-1), 140.0 (C-8), 150.6 (C-4), 165.1 (C-1'), 165.6 (C-1'').

4-((butyryloxy)(phenyl)methyl)phenyl butyrate (**3c**): Yellowish oil. Yield: (0.33 g, 88%). IR ( $\tilde{\nu}/\text{cm}^{-1}$ ): 3024 (Csp<sup>2</sup>-H stretching), 1740 (C=O stretching), 1504, 1206 (C-O stretching), 1157, 746.  $^1\text{H}$  NMR (500 MHz,  $\text{CDCl}_3$ ,  $\delta/\text{ppm}$ ): 0.94 (t,  $J = 7.4$  Hz, 3H, H-4''), 1.03 (t,  $J = 7.4$  Hz, 3H, H-4'), 1.69 (q,  $J = 7.4$  Hz, 2H, H-3''), 1.77 (q,  $J = 7.4$  Hz, 2H, H-3'), 2.40 (t,  $J = 7.4$  Hz, 2H, H-2''), 2.52 (t,  $J = 7.4$  Hz, 2H, H-2'), 6.82 (s, 1H, H-7), 6.97 (d,  $J = 8.6$  Hz, 2H, H-3, H-5), 7.17-7.27 (m, 7H, H-2, H-6, H-9–H-13).  $^{13}\text{C}$  NMR (125 MHz,  $\text{CDCl}_3$ ,  $\delta/\text{ppm}$ ): 13.7 (C-4'), 13.9 (C-4''), 18.4 (C-3', C-3''), 36.3 (C-2'), 36.5 (C-2''), 76.0 (C-7), 121.6 (C-3, C-5), 127.0 (C-9, C-13), 127.9 (C-11), 128.3 (C-2, C-6), 128.5 (C-10, C-12), 137.8 (C-1), 140.1 (C-8), 150.3 (C-4), 172.0 (C-1'), 172.6 (C-1'').

4-((isobutyryloxy)(phenyl)methyl)phenyl isobutyrate (**3d**)<sup>11</sup>: Yellowish oil. Yield: (0.32 g, 86%). IR ( $\tilde{\nu}/\text{cm}^{-1}$ ): 2995 (Csp<sup>2</sup>-H stretching), 1735 (C=O stretching), 1504, 1461, 1195 (C-O stretching), 1151, 750.  $^1\text{H}$  NMR (500 MHz,  $\text{CDCl}_3$ ,  $\delta/\text{ppm}$ ): 1.20 (d,  $J = 7.0$  Hz, 6H, H-3'', H-4''), 1.30 (d,  $J = 7.0$  Hz, 6H, H-3', H-4'), 2.66 (m, 1H, H-2''), 2.78 (m, 1H, H-2'), 6.86 (s, 1H, H-7), 7.04 (d,  $J = 8.6$  Hz, 2H, H-3, H-5), 7.27-7.35 (m, 7H, H-2, H-6, H-9–H-13).  $^{13}\text{C}$  NMR (125 MHz,  $\text{CDCl}_3$ ,  $\delta/\text{ppm}$ ): 18.8 (C-3', C-4'), 18.9 (C-3'', C-4''), 34.1 (C-2'), 34.2 (C-2''), 76.0 (C-7), 121.5 (C-3, C-5), 127.0 (C-9, C-13), 127.9 (C-11), 128.2 (C-2, C-6), 128.5 (C-10, C-12), 137.8 (C-1), 140.1 (C-8), 150.4 (C-4), 175.5 (C-1'), 175.9 (C-1'').

4-(((cyclohexanecarbonyl)oxy)(phenyl)methyl)phenyl cyclohexane carboxylate (**3e**): Yellowish oil. Yield: (0.42 g, 91%). IR ( $\tilde{\nu}/\text{cm}^{-1}$ ): 3021 (Csp<sup>2</sup>-H stretching), 2932 (Csp<sup>3</sup>-H stretching), 1728 (C=O stretching), 1507, 1450, 1209 (C-O stretching), 1160, 746.  $^1\text{H}$  NMR (500 MHz,  $\text{CDCl}_3$ ,  $\delta/\text{ppm}$ ): 1.30 (m, 6H, H-4a', H-6a', H-4a'', H-6a'', H-5a', H-5a''), 1.47 (m, 2H, H-3a', H-7a''), 1.57 (m, 2H, H-3a', H-7a'), 1.66 (m, 2H, 5b', H-5b''), 1.75 (m, 2H, H-4b'', H-6b''), 1.81 (m, 2H, H-4b', H-6b'), 1.95 (m, 2H, H-3b'', H-7b''), 2.04 (m, 2H, H-3b', H-7b'), 2.40 (m, 1H, H-2''), 2.54 (m, 1H, H-2'), 6.86 (s, 1H, H-7), 7.03 (d,  $J = 8.6$  Hz, 1H, H-3, H-5), 7.27-7.33 (m, 7H, H-2, H-6, H-9–H-13).  $^{13}\text{C}$  NMR (125 MHz,  $\text{CDCl}_3$ ,  $\delta/\text{ppm}$ ): 25.3 (C-4', C-6'), 25.4 (C-4'', C-6''), 25.7 (C-5', C-5''), 28.9 (C-3', C-7', C-3'', C-7''), 43.2 (C-2', C-2''), 75.7 (C-7), 121.5 (C-3, C-5), 126.9 (C-9, C-13), 127.9 (C-11), 128.2 (C-2, C-6), 128.5 (C-18, C-12), 137.8 (C-1), 140.2 (C-8), 150.4 (C-4), 174.5 (C-1'), 174.8 (C-1'').

4-(((furan-2-carbonyl)oxy)(phenyl)methyl)phenyl furan-2-carboxylate (**3f**): Brown solid. Yield: (0.35 g, 82%). IR ( $\tilde{\nu}/\text{cm}^{-1}$ ): 3024 (Csp<sup>2</sup>-H stretching), 1725 (C=O stretching), 1513, 1473, 1214 (C-O stretching), 1174, 752.  $^1\text{H}$  NMR (500 MHz,  $\text{CDCl}_3$ ,  $\delta/\text{ppm}$ ): 6.53 (dd,  $J = 3.5, 1.6$  Hz, 1H, H-3'), 6.59 (dd,  $J = 3.6, 1.6$  Hz, 1H, H-4'), 6.61 (dd,  $J = 3.5, 1.6$  Hz, 1H, H-5'), 7.12 (s, 1H, H-7), 7.21 (d,  $J = 8.5$  Hz, 2H, H-3, H-5), 7.31 (t,  $J = 8.2$  Hz, 1H, H-11), 7.37 (t,  $J = 8.2$  Hz, 2H, H-10, H-12), 7.42 (d,  $J = 8.2$  Hz, 2H, H-9, H-13), 7.46 (d,  $J = 8.5$  Hz, 2H, H-2, H-6), 7.61 (d,  $J = 0.7$  Hz, 1H, H-3''), 7.67 (d,  $J = 0.7$  Hz, 1H, H-4''), 7.71 (d,  $J = 0.7$  Hz, 1H, H-5'').  $^{13}\text{C}$  NMR (125 MHz,  $\text{CDCl}_3$ ,  $\delta/\text{ppm}$ ): 76.6 (C-7), 111.9 (C-3'), 112.3 (C-4'), 112.7 (C-5'), 121.7 (C-3, C-5), 127.2 (C-9, C-13), 128.2 (C-11), 128.5 (C-2, C-6), 128.6 (C-10, C-12), 137.8 (C-1), 139.5 (C-8), 143.9 (C-2'), 144.5 (C-2''), 146.8 (C-3''), 147.3 (C-4''), 148.6 (C-5''), 149.9 (C-4), 156.8 (C-1'), 157.7 (C-1'').

Synthesis of benzhydryl analogues, antiproliferative activity and *in silico* studies

## 3.2. Biological Assay

3.2.1 *In-vitro* antiproliferative assay on breast cancer cells

The cytotoxic activities of the tested compounds against cultured cell lines have been expressed as the IC<sub>50</sub> values in  $\mu\text{M}$  and as well as selective index (SI). The lower value of IC<sub>50</sub> indicates stronger inhibition of cell proliferation. The IC<sub>50</sub> values of the compounds against these human cancer cells are summarized in Table 1.

**Table 1.** The IC<sub>50</sub> value of benzhydryl analogues **3a-3f**

Compounds	Anti-proliferative IC <sub>50</sub> $\mu\text{M}$ (Mean $\pm$ SD)					
	Time	MCF-7	SI	MDA-MB-231	SI	MCF-10
<b>3a</b>	24h	>100	-	>100	-	>100
	48h	>100	-	>100	-	>100
	72h	77.05 $\pm$ 2.55	1.30	60.01 $\pm$ 3.56	1.66	>100
<b>3b</b>	24h	18.25 $\pm$ 1.85	1.27	41.43 $\pm$ 4.59	0.56	23.35 $\pm$ 0.26
	48h	9.78 $\pm$ 0.30	1.67	15.84 $\pm$ 1.01	1.03	16.38 $\pm$ 2.19
	72h	5.50 $\pm$ 2.88	3.16	1.19 $\pm$ 0.78	14.65	17.43 $\pm$ 2.23
<b>3c</b>	24h	>100	0.23	33.62 $\pm$ 0.47	0.67	22.86 $\pm$ 0.59
	48h	81.99 $\pm$ 6.42	0.35	24.41 $\pm$ 0.24	1.17	28.46 $\pm$ 0.06
	72h	30.47 $\pm$ 0.54	0.65	21.78 $\pm$ 1.00	0.90	19.68 $\pm$ 0.10
<b>3d</b>	24h	61.78 $\pm$ 1.19	0.42	29.68 $\pm$ 4.90	0.88	26.18 $\pm$ 0.60
	48h	35.17 $\pm$ 0.39	0.65	7.47 $\pm$ 0.86	3.07	22.98 $\pm$ 0.38
	72h	14.55 $\pm$ 0.05	1.31	4.99 $\pm$ 0.52	3.83	19.12 $\pm$ 0.21
<b>3e</b>	24h	21.40 $\pm$ 1.99	5.83	49.41 $\pm$ 3.25	2.53	124.77 $\pm$ 2.73
	48h	7.07 $\pm$ 0.28	13.49	37.72 $\pm$ 2.46	2.52	95.34 $\pm$ 4.93
	72h	6.03 $\pm$ 0.41	17.68	9.19 $\pm$ 0.23	11.6	106.67 $\pm$ 8.20
<b>3f</b>	24h	22.57 $\pm$ 0.86	1.24	11.91 $\pm$ 0.34	2.36	28.13 $\pm$ 1.36
	48h	17.46 $\pm$ 0.95	0.90	12.55 $\pm$ 0.77	1.26	15.87 $\pm$ 0.16
	72h	5.63 $\pm$ 0.35	2.67	7.09 $\pm$ 0.48	2.12	15.03 $\pm$ 1.59
<b>Tamoxifen (control)</b>	24h	17.22 $\pm$ 0.37	0.19	13.62 $\pm$ 0.95	0.24	3.24 $\pm$ 0.01
	48h	15.35 $\pm$ 1.42	0.21	15.86 $\pm$ 0.73	0.21	3.33 $\pm$ 9.02
	72h	15.78 $\pm$ 0.10	0.26	14.53 $\pm$ 0.08	0.28	4.07 $\pm$ 0.09

\*Results are expressed as mean  $\pm$  SD (n=3) of at least three independent experiments.

All the tested compounds exhibited cytotoxicity activities with IC<sub>50</sub> values in the range of 1.19 to 100  $\mu\text{M}$ . Compounds **3b** and **3e** showed IC<sub>50</sub> values in the range of 5-9  $\mu\text{M}$ , respectively for 48 and 72 hrs against MCF-7, which were found to possess higher cytotoxicity than the positive control (tamoxifen). Meanwhile, **3b** at 48 and 72 hr respectively displayed IC<sub>50</sub> values of 15.84 $\pm$ 1.01 and 1.19 $\pm$ 0.78  $\mu\text{M}$  against non-hormonal breast cancer (MDA-MB-231) and compound **3e**, displayed moderate cytotoxicity activity when compared with tamoxifen as shown in Table 1. The presence of the benzene ring in **3b** and the presence of cyclohexane ring in **3e** attached to the benzhydryl core skeleton might responsible for the anticancer activity of both compounds.

The presence of the furan ring which acts as an electron donor attached to the benzhydryl core skeleton in compound **3f** revealed its potent cytotoxicity at 72 hr with IC<sub>50</sub> values of 5.63 $\pm$ 0.35  $\mu\text{M}$  and 7.09 $\pm$ 0.48  $\mu\text{M}$  against MCF-7 and MDA-MB-231, respectively when compared with tamoxifen. Furthermore, **3a** and **3c** showed moderate cytotoxicity in both cell lines when compared with positive control at different time intervals. Meanwhile, **3d** displayed a good selectivity towards MDA-MB-231 with IC<sub>50</sub> values of 7.47 $\pm$ 0.86  $\mu\text{M}$  and 4.99 $\pm$ 0.53  $\mu\text{M}$  for 48 and 72 hr, respectively when compared with other derivatives and tamoxifen.

Tamoxifen also was found to be cytotoxic to normal breast cell lines with IC<sub>50</sub> values of 15.35  $\pm$  1.42  $\mu\text{M}$  after 24 hr of subjection. This finding showed similar reported work by Bakar *et al.* (2023) whereby tamoxifen was found to be toxic towards cancerous and non-cancerous cells at  $\mu\text{M}$  concentration which might be due to the presence of estrogen receptors.<sup>17</sup> Additionally, tamoxifen showed impressive cytotoxic activity towards MDA-MB231 with IC<sub>50</sub> values of 15.86  $\pm$  0.73  $\mu\text{M}$  after 24 hr.



This trend suggested that the cytotoxicity of tamoxifen probably involves more than one pathway, which included one pathway of the estrogen receptor-independent and another pathway of the estrogen receptor-dependent. However, MCF-7 is a breast cancer cell line associated with hormone receptors such as estrogen and progesterone.<sup>18</sup> The hormonal breast cancer type is most likely found in non-metastatic cancer, which is relatively able to be stopped using common anti-breast cancer drugs such as tamoxifen.<sup>19</sup> In contrast, the non-hormonal cancer type such as MDA-MB-231 was not too sensitive against tamoxifen due to its metastatic character.<sup>18</sup> Therefore, most active compounds have selectively inhibited the non-metastatic cancer cell rather than the metastatic cancer cell. However, the results showed that the most active compounds, **3b** and **3e**, were slightly better than tamoxifen in inhibiting the non-metastatic cancer cell that could be a potential agent for breast anticancer and **3d** could be a potential target compound against negative breast cancer.

The SI value was obtained by dividing the IC<sub>50</sub> value for normal cell lines by the IC<sub>50</sub> for cancerous cell lines. All compounds with SI values less than 2 were considered to have general toxicity, suggesting that they can cause cytotoxicity in normal cells as well.<sup>20</sup> Based on this, the SI data shown in Table 1 indicates that compound **3b**, **3d**, **3e** and **3f** showed a high degree of cytotoxic selectivity against MCF-7 and MDA-MB-231, which exhibited an increased cytotoxic selectivity than the positive control at different time interval (24-72 hr). On the other hand, compounds **3a** and **3c** exhibited a lower degree of cytotoxic selectivity against MCF-7 and MDA-MB-231, showing an increased cytotoxicity toward the healthy cell.

### 3.3. ADMET and Toxicity Profiles Prediction

To enhance the efficiency of experimental efforts and improve the success rate in identifying potential drug candidates, we initially utilized SwissADME to predict the pharmacokinetics of novel ACA analogs. This tool provides fundamental information on the molecular properties and pharmacokinetic activity that resemble drug-like characteristics. Lipinski's rule of five, a widely accepted guideline for preliminary drug-likeness screening, outlines the parameters for oral absorption or permeation of a drug. According to this rule, a potential drug candidate should have a molecular weight (MW) less than 500 g/mol, lipophilicity (Log P) less than 4.15, fewer than 5 H-bond donors, and fewer than 10 H-bond acceptors. Additionally, the total polar surface area (TPSA) should be less than 140 Å<sup>2</sup>, and the number of rotatable bonds should be less than 10.<sup>21</sup> Based on the data presented in Table 2, only **3d** and **3f**, adhere to all Lipinski's rule of five, while **3b** and **3e** with one violation of Log P greater than 4.15, making them suitable candidate drugs against IκBα

The TPSA of the newly synthesized ACA analogs, which ranges from 52.60 to 78.88 Å<sup>2</sup>, plays a significant role in their high gastrointestinal (GI) absorption prediction. This aligns with the findings of Simon *et al.*, demonstrated that ACA is well absorbed through the gastrointestinal tract, a fact that was confirmed using an *in vitro* assay. Furthermore, the newly synthesized compounds (**3b** and **3d**) have the ability to penetrate the blood-brain barrier, similar to their parent compound, ACA.<sup>22</sup> The CYP isoenzymes play a crucial role in the biotransformation of drugs. The metabolic process of drugs through CYP isoenzymes can result in drug toxicities and a reduced pharmacological impact.<sup>23</sup> It was predicted that **3d** and **3f** would not act as substrates for P-gp. Both of these compounds were forecasted to inhibit CYP1A2 and CYP2C19. On the other hand, **3b** was anticipated to inhibit CYP2C19 and CYP2C9, while **3e** was expected to act as an inhibitor for CYP2C9, CYP2D6, and CYP3A4. It is predicted that **3e** will inhibit extensive metabolism by CYP3A4, leading to favorable pharmacokinetics, similar to the action of ritonavir.<sup>24</sup> These predictions suggest that the biotransformation of the compounds will occur through the CYP isoenzymes.

The potential toxic effects of the newly developed ACA analogues (**3b**, **3d**, **3e**, and **3f**) were estimated using a freely accessible computational tool ([https://tox-new.charite.de/protox\\_II/](https://tox-new.charite.de/protox_II/)). The software provided predictions on the organ toxicity of these compounds, suggesting their potential to cause liver failure (hepatotoxicity), promote tumor growth (carcinogenicity), trigger unusual genetic changes (mutagenicity), inflict unwanted cellular damage (cytotoxicity), induce harmful effects on the immune system due to foreign substances (immunotoxicity) and the involvement in toxicology pathway via stress response pathway (phosphoprotein tumor suppressor (p53)).<sup>14</sup>

Synthesis of benzhydryl analogues, antiproliferative activity and *in silico* studies

The compounds did not reveal the capability to induce organ toxicity except compounds **3b** and **3e** which revealed the capability to induce hepatotoxicity which could be attributed to the addition of phenyl and cyclohexyl in R1 position. Drugs that exhibit a high degree of lipophilicity, characterized by a Log P value greater than 5, tend to be metabolized rapidly. They also typically demonstrate poor solubility and are not easily absorbed. The elevated lipophilicity contributes to both toxicity and metabolic clearance.<sup>25</sup> Moreover, both **3b** and **3e** show that they can be transported across both extracellular and intracellular membranes of the intestinal lumen and capillary endothelial cells, leading to their clearance.

**Table 2.** ADMET parameters of **3b**, **3d**, **3e**, and **3f** compounds

ADMET	Compound			
	<b>3b</b>	<b>3d</b>	<b>3e</b>	<b>3f</b>
<i>Physicochemical properties</i>				
Formula	C <sub>27</sub> H <sub>20</sub> O <sub>4</sub>	C <sub>19</sub> H <sub>20</sub> O <sub>4</sub>	C <sub>27</sub> H <sub>32</sub> O <sub>4</sub>	C <sub>23</sub> H <sub>16</sub> O <sub>6</sub>
Molecular weight	408.45 g/mol	312.36 g/mol	420.54 g/mol	388.37 g/mol
Num. heavy atoms	31	23	31	29
Num. arom. heavy atom	24	12	12	22
Num. rotatable bonds	8	7	8	8
Num. H-bond acceptors	4	4	4	6
Num. H-bond donors	0	0	0	0
Molar Refractivity	118.10	87.91	122.14	102.63
TPSA	52.60 Å <sup>2</sup>	52.60 Å <sup>2</sup>	52.60 Å <sup>2</sup>	78.88 Å <sup>2</sup>
<i>ADME</i>				
Water solubility	Poorly soluble	Moderately soluble	Poorly soluble	Moderately soluble
GI absorption	High	High	High	High
BBB permeant	Yes	Yes	No	No
P-gp substrate	Yes	No	Yes	No
CYP1A2 inhibitor	No	Yes	No	Yes
CYP2C19 inhibitor	Yes	Yes	No	Yes
CYP2C9 inhibitor	Yes	No	Yes	Yes
CYP2D6 inhibitor	No	No	Yes	No
CYP3A4 inhibitor	No	No	Yes	No
Log Kp (skin permeation)	-4.27 cm/s	-5.29 cm/s	-3.74 cm/s	-5.00 cm/s
Lipinski	Yes; 1 violation: MLOGP>4.15	Yes; 0 violation	Yes; 1 violation: MLOGP>4.15	Yes; 0 violation
Ghose	Yes	Yes	No; 1 violation: WLOGP>5.6	Yes
Veber	Yes	Yes	Yes	Yes
Egan	Yes	Yes	No; 1 violation: WLOGP>5.88	Yes
Muegge	No; 1 violation: XLOGP3>5	Yes	No; 1 violation: XLOGP3>5	No; 1 violation: XLOGP3>5
<i>Prediction of toxicity</i>				
Carcinogenicity	Inactive (73%)	Inactive (72%)	Inactive (67%)	Active (55%)
Immunotoxicity	Inactive (99%)	Inactive (96%)	Inactive (99%)	Inactive (99%)
Mutagenicity	Inactive (92%)	Inactive (89%)	Inactive (88%)	Inactive (82%)
Cytotoxicity	Inactive (90%)	Inactive (80%)	Inactive (86%)	Inactive (82%)
Phosphoprotein (Tumor Suppressor) p53	Inactive (97%)	Inactive (82%)	Inactive (95%)	Inactive (91%)
Hepatotoxicity	Active (52%)	Inactive (50%)	Active (56%)	Inactive (62%)

### 3.4. Molecular Docking Studies

Aun et al. demonstrated that 1'S-1'-acetoxyeugenol acetate (AEA), derived from the rhizomes of *A. conchigera*, can enhance apoptosis in MCF-7 cells. This is evidenced by the downregulation of several gene targets, including I $\kappa$ B $\alpha$ , that are regulated by NF- $\kappa$ B.<sup>8</sup> Jacobs and Harrison (1998) demonstrated that residues of N-terminal of I $\kappa$ B $\alpha$  important for the interaction with p65 of NF- $\kappa$ B.<sup>26</sup> To further investigate the interaction of the newly synthesized compound, molecular docking analysis was performed using the identified area as the surface pocket. As depicted in Table 3, the binding energies corresponding to various compounds in relation to the I $\kappa$ B $\alpha$  protein are presented. The binding energy serves as an indicator of the intensity of interaction between the compound and the protein. An inverse relationship is observed, where a lower binding energy signifies a stronger interaction between the compound and the protein.<sup>27</sup>

In the study, compound **3a** demonstrated a binding energy of -5.13 kcal/mol, with a standard deviation of  $\pm 0.115$ . Compound **3b** exhibited a stronger interaction, reflected by a lower binding energy of -7.27 kcal/mol ( $\pm 0.058$ ). The binding energy for compound **3c** was found to be -5.23 kcal/mol ( $\pm 0.252$ ), whereas compound **3d** displayed a marginally stronger interaction with a binding energy of -5.57 kcal/mol ( $\pm 0.153$ ). Interestingly, compound **3e** mirrored the binding energy of compound **3b**, both registering the strongest binding energy of -7.03 kcal/mol ( $\pm 0.058$ ). Compound **3f** showed a binding energy of -6.47 kcal/mol ( $\pm 0.306$ ). For comparison, tamoxifen, employed as a control in this experiment, recorded a binding energy of -5.27 kcal/mol ( $\pm 0.058$ ). These findings provide valuable insights into the binding affinities of these compounds with the target protein, I $\kappa$ B $\alpha$ .

**Table 3.** Compound binding energy result of docking against I $\kappa$ B $\alpha$

Protein	Compound	Binding Energy (kcal/mol)
I $\kappa$ B $\alpha$ (PDB ID: 1NFI)	3a	-5.13 $\pm$ 0.115
	3b	-7.27 $\pm$ 0.058
	3c	-5.23 $\pm$ 0.252
	3d	-5.57 $\pm$ 0.153
	3e	-7.03 $\pm$ 0.058
	3f	-6.47 $\pm$ 0.306
	Tamoxifen (control)	-5.27 $\pm$ 0.058

Both compounds **3b** and **3e** interact with the protein I $\kappa$ B $\alpha$  at similar residues (Figure 3a). These include PHE77, VAL93, VAL97, and PHE103 (Table 4 and Figure 3). However, the nature of these interactions differs between the two compounds. For compound **3b**, the phenyl group forms a  $\pi$ -alkyl interaction with PHE77, VAL93, VAL97, a  $\pi$ - $\pi$  T-shaped interaction with PHE103, a carbon H-bond between =O of **3b** and PHE77, as well as  $\pi$ -sigma and  $\pi$ - $\pi$  stacked interactions with PHE77. The binding energy of compound **3b** with I $\kappa$ B $\alpha$  is -7.27  $\pm$  0.058 kcal/mol, indicating a relatively strong interaction. On the other hand, compound **3e** forms an alkyl interaction with VAL3 and VAL97, and a H-bond between =O of **3e** and THR71 and PHE77. It also forms a  $\pi$ -alkyl interaction with PHE77 and PHE103. The binding energy of compound **3e** with I $\kappa$ B $\alpha$  is -7.03  $\pm$  0.058 kcal/mol, which is slightly less than that of compound **3b**, indicating a slightly weaker interaction than **3b**.

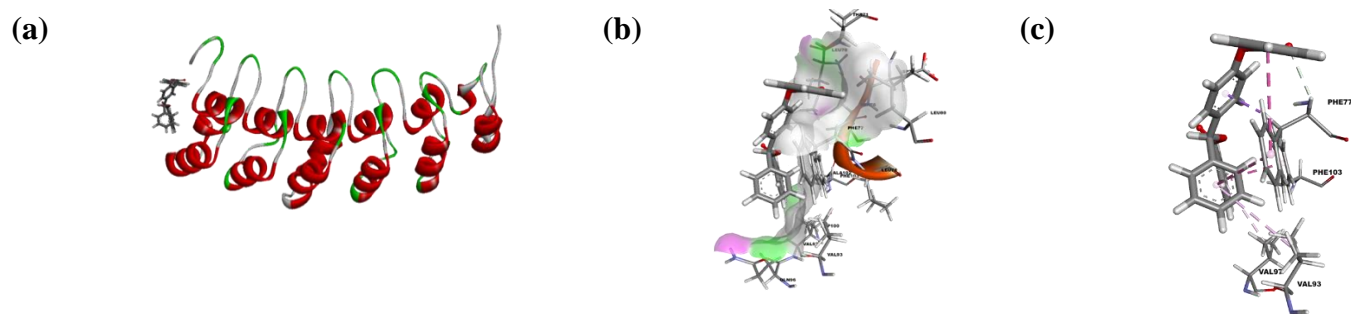
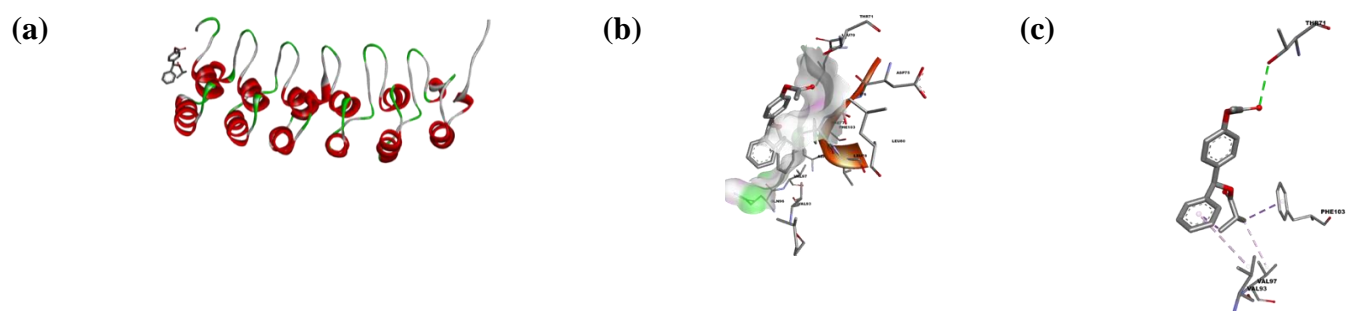
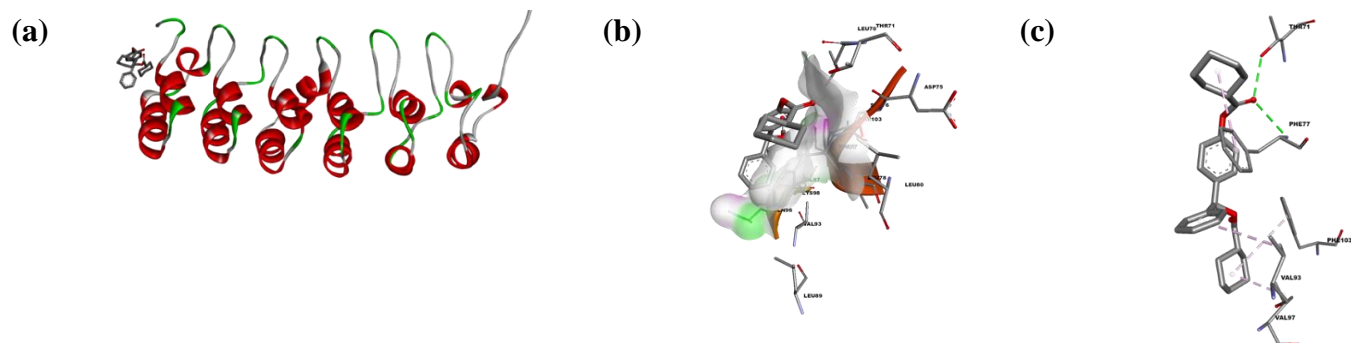
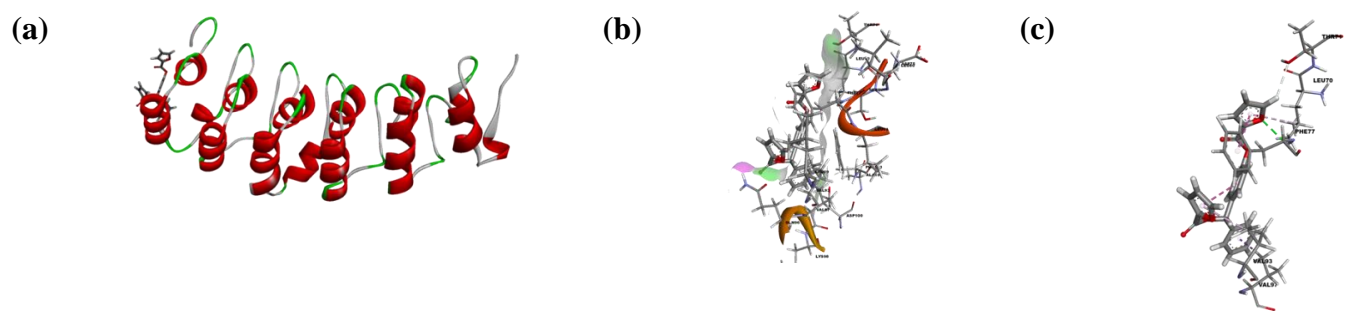
Compound **3d** interacts with the protein residues THR71, VAL93, VAL97, and PHE103 using =O, phenyl, and methyl as interaction units, and exhibits carbon H-bond, alkyl,  $\pi$ -alkyl and  $\pi$ -sigma types of interactions. On the other hand, compound **3f** interacts with the protein residues THR71, using CH for forming a carbon H-bond interaction. LEU70, PHE77, VAL93, and VAL97 using =O, and phenyl as interaction units, and exhibits H-bond, alkyl,  $\pi$ -alkyl,  $\pi$ - $\pi$  stacked and  $\pi$ -sigma types of interactions. For tamoxifen, the protein residues involved are VAL93, GLN96, VAL97, and PHE103. The interaction units of the compound mostly phenyl and methyl. The types of interactions include carbon H-bond,  $\pi$ -alkyl and  $\pi$ - $\pi$  T-shaped (Table 4).

Synthesis of benzhydryl analogues, antiproliferative activity and *in silico* studies

Although tamoxifen exhibits a weaker binding energy (-5.27), however, one of its phenyl units interacts with GLN96 of I $\kappa$ B $\alpha$  that is important in the binding between I $\kappa$ B $\alpha$  and p65 of NF- $\kappa$ B protein.<sup>26</sup> In this study, the newly generated compounds demonstrate ability to interact with I $\kappa$ B $\alpha$  residues and may affect the regulation of NF- $\kappa$ B protein in cancer cells. Other than NF- $\kappa$ B protein, I $\kappa$ B $\alpha$  also can establish interaction with Aurora kinases A (AURKA) and blocking of the complex by small molecule inhibitor known as AKCI exerted antitumor activity in MDA-MB-231 breast cancer cells.<sup>28</sup> Furthermore, Carra and co-worker reported a compound that targets I $\kappa$ B $\alpha$  increased the sensitivity of lung cancer cells to cisplatin, resulting in cell death induced by reactive oxygen species (ROS).<sup>29</sup>

**Table 4.** Binding of compound **3b**, **3d**, **3e**, **3f** and tamoxifen with I $\kappa$ B $\alpha$ 

Protein	Compound	Protein residue	Interaction unit of compounds	Type of interaction				
I $\kappa$ B $\alpha$ (PDB ID: 1NFI)	3b	PHE77	Phenyl	$\pi$ -alkyl				
				$\pi$ -sigma				
				$\pi$ - $\pi$ stacked				
			3d	PHE103	Phenyl	=O	Carbon H-bond	
						VAL93	Phenyl	$\pi$ -alkyl
						VAL97	Phenyl	$\pi$ -alkyl
						THR71	=O	Carbon H-bond
						VAL93	Phenyl	alkyl
						VAL97	Methyl	$\pi$ -alkyl
						PHE103	Methyl	$\pi$ -sigma
	3e	PHE103	Phenyl	=O	H-bond			
				THR71	=O	H-bond		
				VAL93	Phenyl	$\pi$ -alkyl		
				VAL97	Phenyl	alkyl		
				PHE103	Phenyl	alkyl		
	3f	PHE103	Phenyl	CH	Carbon H-bond			
				LEU70	Phenyl	$\pi$ -alkyl		
				PHE77	O	H-bond		
				Phenyl	$\pi$ -alkyl			
				Phenyl	$\pi$ - $\pi$ stacked			
				Phenyl	$\pi$ - $\pi$ stacked			
				VAL93	Phenyl	$\pi$ -alkyl		
				VAL97	Phenyl	$\pi$ -sigma		
Tamoxifen				PHE103	Phenyl	VAL93	Carbon H-bond	
						GLN96	Phenyl	$\pi$ -alkyl
	VAL97	Phenyl	$\pi$ -alkyl					
	Methyl	$\pi$ -alkyl						
	PHE103	Phenyl	$\pi$ - $\pi$ T-shaped					

**Compound 3b - I $\kappa$ B $\alpha$  complex****Compound 3d - I $\kappa$ B $\alpha$  complex****Compound 3e - I $\kappa$ B $\alpha$  complex****Compound 3f - I $\kappa$ B $\alpha$  complex**

**Figure 3.** 3D molecular structure of protein-ligand binding of compound **3b**, **3d**, **3e**, **3f** and tamoxifen (control) against protein I $\kappa$ B $\alpha$ . (a) I $\kappa$ B $\alpha$  – Compound Complex (b) Pocket Surface (c) 3D Structure Interaction (*continued..*)

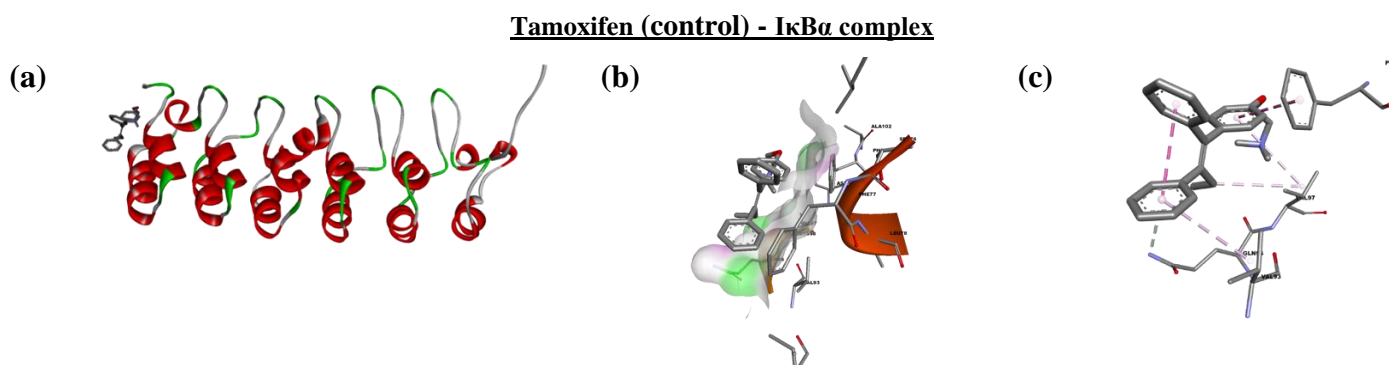


**Figure 3.** 3D molecular structure of protein-ligand binding of compound **3b**, **3d**, **3e**, **3f** and tamoxifen (control) against protein I $\kappa$ B $\alpha$ . (a) I $\kappa$ B $\alpha$  – Compound Complex (b) Pocket Surface (c) 3D Structure Interaction.

#### 4. Conclusion

In conclusion, we managed to develop the stable and more potent antiproliferative compounds (i.e. **3b**, **3e**, and **3f**) by the structural modification of 1'-acetoxychavicol acetate (ACA) and 1'-acetoxyeugenol acetate (AEA). These compounds exhibited varying levels of cytotoxic selectivity against the MCF-7 and MDA-MB-231 human breast cancer cell lines. Our findings suggest compounds **3b**, **3d**, **3e**, and **3f** are promising candidates for selective antiproliferative activity, while **3a** and **3c** may pose higher risks of toxicity to non-cancerous cells. Molecular docking studies further supported these findings, demonstrating that these compounds have strong binding affinities with the Nuclear Factor-KappaB Kinase alpha (I $\kappa$ B $\alpha$ ) protein, with binding energies between -5.13 to -7.27 kcal/mol, compared to -5.27 kcal/mol for tamoxifen (control). Future research should focus on detailed mechanistic studies and *in vivo* evaluations to further explore their therapeutic potential.

#### Acknowledgements

The author would like to acknowledge the financial support from the Ministry of Higher Education Malaysia (MOHE) under the Fundamental Grant Research Scheme (FRGS) - FRGS/1/2023/STG04/USM/02/3. The authors sincerely thank University Sains Malaysia (USM) for approval of sabbatical leave M.N.A. and the NPSO Laboratory for the facilities used in this research work.

#### Supporting Information

Supporting information accompanies this paper at <http://www.acgpubs.org/journal/organic-communications>

#### ORCID

Mohamad Nurul Azmi: [0000-0002-2447-0897](https://orcid.org/0000-0002-2447-0897)

Cheong Siong Tan: [0009-0002-7415-6094](https://orcid.org/0009-0002-7415-6094)

Hassan Taiye Abdulameed: [0000-0001-6336-0407](https://orcid.org/0000-0001-6336-0407)

Nik Nur Syazni Nik Mohamad Kamal: [0000-0001-5473-1245](https://orcid.org/0000-0001-5473-1245)

Nur Ezzah Abdul Kahar: [0000-0001-6614-4822](https://orcid.org/0000-0001-6614-4822)

Mohammad Tasyriq Che Omar: [0000-0002-1294-7520](https://orcid.org/0000-0002-1294-7520)

## References

- [1] World Health Organization. Global cancer observatory: *Cancer Today* 2024, May 12.
- [2] Feng, Y.; Spezia, M.; Huang, S.; Yuan, C.; Zeng, Z.; Zhang, L.; Ji, X.; Liu, W.; Huang, B.; Luo, W.; Liu, B.; Lei, Y.; Du, S.; Vuppalapati, A.; Luu, H. H.; Haydon, R. C.; He, T.; Ren, G. Breast cancer development and progression: Risk factors, cancer stem cells, signaling pathways, genomics, and molecular pathogenesis. *Genes. Dis.* **2018**, *5*, 77–106.
- [3] Liew, S. K.; Azmi, M. N.; In, L. L.; Awang, K.; Nagoor, N. H. Anti-proliferative, apoptotic induction, and 1'S-1'-acetoxychavicol acetate analogs on MDA-MB-231 breast cancer cells. *Drug. Des. Devel. Ther.* **2017**, *11*, 2763–2776.
- [4] Awang, K.; Azmi, M. N.; In, L. L.; Aziz, A. N.; Ibrahim, H.; Nagoor, N. H. The apoptotic effect of 1'S-1'-acetoxychavicol acetate from *Alpinia conchigera* on human cancer cells. *Molecules.* **2010**, *15*, 8048-8059.
- [5] Akiko, K. Y.; Isao, M. Y. Pharmacological effects of 1'-acetoxychavicol acetate, a major constituent in the rhizomes of *Alpinia galanga* and *Alpinia conchigera*. *J. Med. Food.* **2020**, 1-11.
- [6] Guang, H. O.; Daisuke, O.; Takumi, K.; Taro, K. Inhibition of lipopolysaccharide-induced inflammatory responses by 1'-acetoxychavicol acetate. *Genes. Cells.* **2022**, *27*(7), 482-492.
- [7] In, L. L.; Azmi, M. N.; Ibrahim, H.; Awang, K.; Nagoor, N. H. 1'S-1'-acetoxychavicol acetate: A novel phenylpropanoid from *Alpinia conchigera* enhances the apoptotic effects of paclitaxel in MCF-7 cells through NF- $\kappa$ B inactivation. *Anti-Cancer Drugs.* **2011**, *22*, 424-434.
- [8] In, L. L.; Mohd Arshad, N.; Ibrahim, H.; Azmi, M. N.; Awang, K.; Nagoor, N. H. 1'-Acetoxychavicol acetate inhibits growth of human oral carcinoma xenograft in mice and potentiates cisplatin effect via proinflammatory microenvironment alterations. *BMC Complement Altern. Med.* **2012**, *12*, 179.
- [9] Ryosuke, S.; Naoya, H.; Ami, Y.; Yuki, K.; Fumihiko, I.; Teruaki, T.; Genzoh, T.; Reiko, S. Discovery of new benzhydrol biscarbonate esters as potent and selective apoptosis inducers of human melanomas bearing the activated ERK pathway: SAR studies on an ERK MAPK signaling modulator, ACA-28. *Bioorg. Chem.* **2020**, *103*, 104137.
- [10] Tomohisa, Y.; Yoshiaki, M.; Takayuki, M.; Wang, Q.; Hisashi, M.; Masayuki, Y.; Osamu, M. Acetoxybenzhydrols as highly active and stable analogues of 1'S-1'-acetoxychavicol, a potent antiallergic principal from *Alpinia galanga*. *Bioorg. Med. Chem. Lett.* **2009**, *19*(11), 2944-2946.
- [11] Chagas, C. M.; Moss, S.; Alisarai, L. Drug metabolites and their effects on the development of adverse reactions: Revisiting Lipinski's rule of five. *Int. J. Pharm.* **2018**, *549*, 133–149.
- [12] Daina, A.; Michielin, O.; Zoete, V. SwissADME: a free web tool to evaluate pharmacokinetics, drug-likeness and medicinal chemistry friendliness of small molecules. *Sci. Rep.* **2017**, *7*, 42717.
- [13] Banerjee, P.; Eckert, A. O.; Schrey, A. K.; Preissner, R. ProTox-II: a webserver for the prediction of toxicity of chemicals. *Nucleic Acid. Res.* **2018**, *46*(W1), W257–W263.
- [14] Pettersen, E. F.; Goddard, T. D.; Huang, C. C.; Couch, G. S.; Greenblatt, D. M.; Meng, E. C.; Ferrin, T. E. UCSF Chimera—a visualization system for exploratory research and analysis. *J. Comput. Chem.* **2004**, *25*(13), 1605.
- [15] Huang, C. C.; Meng, E. C.; Morris, J. H.; Pettersen, E. F.; Ferrin, T. E. Enhancing UCSF Chimera through web services. *Nucleic Acids Res.* **2014**, *42*(W1), W478-484.
- [16] Bakar, B. I.; Alidmat, M. M.; Khairuddean, M.; Ibrahim, W. N. A. W.; Mun, K. W.; Kamal, N. N. S. N. M.; Muhammad, M. Synthesis, characterization, cytotoxicity evaluation and molecular docking study of new bis-chalcone, fused-pyrimidine and fused-pyrazoline derivatives. *Indian J. Chem.* **2023**, *62*(3), 251-264.
- [17] Holliday, D. L.; Speirs, V. Choosing the right cell line for breast cancer research. *Breast Cancer Res.* **2011**, *13*, 1-7.
- [18] Roviello, G.; Gatta Michelet, M. R.; D'Angelo, A.; Nobili, S.; Mini, E. Role of novel hormonal therapies in the management of non-metastatic castration-resistant prostate cancer: A literature-based meta-analysis of randomized trials. *Clin. Transl. Oncol.* **2020**, *22*, 1033-1039.
- [19] Tan, A. S.; Singh, J.; Rezali, N. S.; Muhamad, M.; Nik Mohamed Kamal, N. N. S.; Six, Y.; Azmi, M. N. Synthesis of bio-inspired 1, 3-diarylpropene derivatives via Heck cross-coupling and cytotoxic evaluation on breast cancer cells. *Molecules* **2022**, *27*(17), 5373.
- [20] Jia, C. Y.; Li, J. Y.; Hao, G. F.; Yang, G. F. A drug-likeness toolbox facilitates ADMET study in drug discovery. *Drug Discov Today.* **2020**, *25*(1), 248–258.
- [21] Simon, A.; Nghiem, K. S.; Gampe, N.; Garádi, Z.; Boldizsár, I.; Backlund, A.; Darcsi, A.; Nedves, A. N.; Riethmüller, E. Stability study of *Alpinia galanga* constituents and investigation of their membrane permeability by ChemGPS-NP and the parallel artificial membrane permeability assay. *Pharmaceutics.* **2022**, *14*(9), 1967.

Synthesis of benzhydrol analogues, antiproliferative activity and *in silico* studies

- [22] Sychev, D. A.; Ashraf, G. M.; Svistunov, A. A.; Maksimov, M. L.; Tarasov, V. V.; Chubarev, V. N.; Otdelenov, V. A.; Denisenko, N. P.; Barreto, G. E.; Aliev, G. The cytochrome P450 isoenzyme and some new opportunities for the prediction of negative drug interaction *in vivo*. *Drug. Des. Devel. Ther.* **2018**, *12*, 1147–1156.
- [23] Shanu-Wilson, J.; Evans, L.; Wrigley, S.; Steele, J.; Atherton, J.; Boer, J. Biotransformation: Impact and application of metabolism in drug discovery. *ACS Med. Chem. Lett.* **2020**, *11*(11), 2087–2107.
- [24] Miller, R. R.; Madeira, M.; Wood, H. B.; Geissler, W. M.; Raab, C. E.; Martin, I. J. Integrating the impact of lipophilicity on potency and pharmacokinetic parameters enables the use of diverse chemical space during small molecule drug optimization. *J. Med. Chem.* **2020**, *63*(21), 12156–12170.
- [25] Jacobs, M. D.; Harrison, S. C. Structure of an IkappaBalpha/NF-kappaB complex. *Cell.* **1998**, *95*(6), 749–58.
- [26] Ivanova, L.; Karelson, M. The impact of software used and the type of target protein on molecular docking accuracy. *Molecules* **2022**, *27*(24), 9041.
- [27] Han, E. H.; Min, J. Y.; Yoo, S. A.; Park, S. J.; Choe, Y. J.; Yun, H. S.; Lee, Z. W.; Jin, S. W.; Kim, H. G.; Jeong, H. G.; Kim, H. K.; Kim, N. D.; Chung, Y. H. A small-molecule inhibitor targeting the AURKC-IkBa interaction decreases transformed growth of MDA-MB-231 breast cancer cells. *Oncotarget.* **2017**, *8*(41), 69691–69708.
- [28] Carrà, G.; Ermondi, G.; Riganti, C.; Righi, L.; Caron, G.; Menga, A.; Capelletto, E.; Maffeo, B.; Lingua, M. F.; Fusella, F.; Volante, M.; Taulli, R.; Guerrasio, A.; Novello, S.; Brancaccio, M.; Piazza, R.; Morotti, A. IkBa targeting promotes oxidative stress-dependent cell death. *J. Exp. Clin. Cancer. Res.* **2021**, *40*(1), 136.

**A C G**  
**publications**

© 2024 ACG Publications